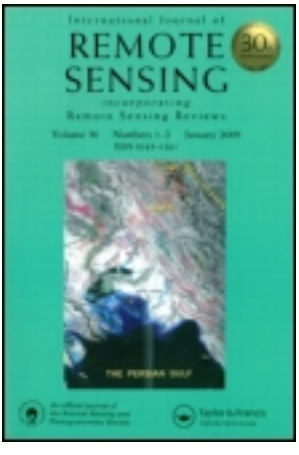

International Journal of Remote Sensing
Publication details, including instructions for authors and subscription information:
http://www.tandfonline.com/loi/tres20

Spectral indices for estimating photosynthetic pigment concentrations: A test using senescent tree leaves

G. A. Blackburn
Published online: 25 Nov 2010.

To cite this article: G. A. Blackburn (1998) Spectral indices for estimating photosynthetic pigment concentrations: A test using senescent tree leaves, International Journal of Remote Sensing, 19:4, 657-675, DOI: 10.1080/014311698215919

To link to this article: http://dx.doi.org/10.1080/014311698215919

INT. J. REMOTE SENSING, 1998, VOL. 19, NO. 4, 657–675

Spectral indices for estimating photosynthetic pigment concentrations: a test using senescent tree leaves

G. A. BLACKBURN

Department of Geography, King's College London, Strand, London WC2R 2LS, England, U.K.

(*Received 25 July 1996; in final form 13 May 1997*)

Abstract. The possibility of estimating the concentration of individual photosynthetic pigments within vegetation from reflectance spectra offers great promise for the use of remote sensing to assess physiological status, species type and productivity. This study evaluates a number of spectral indices for estimating pigment concentrations at the leaf scale, using samples from deciduous trees at various stages of senescence. Two new indices (PSSR and PSND) are developed which have advantages over previous techniques. The optimal individual wavebands for pigment estimation are identified empirically as 680 nm for chlorophyll *a*, 635 nm for chlorophyll *b* and 470 nm for the carotenoids. These wavebands are justified theoretically and are shown to improve the performance of many of the spectral indices tested. Strong predictive models are demonstrated for chlorophyll *a* and *b*, but not for the carotenoids and the paper explores the reasons for this.

1. Introduction

While it has long been known that photosynthetic pigments control the visible reflectance properties of leaves, only recently have techniques been developed to estimate the concentrations of individual pigments within leaves using high spectral resolution (hyperspectral) reflectance measurements (e.g., Chappelle *et al*. 1992, Peñuelas *et al*. 1995). The absolute and relative concentrations of pigments dictate the photosynthetic potential of a leaf and relate strongly to its physiological status. If applied to data from the future generation of space-borne imaging spectrometers such techniques would facilitate an improved interpretation of dynamic physiological processes within terrestrial ecosystems. However, before this is possible it is essential that we investigate the relative merits of different hyperspectral measures of pigment concentrations for different species of plant and at a range of scales, from the individual leaf to the whole canopy.

2. Background

2.1. *Significance of the concentration of individual pigments*

Within the photosynthetically active radiation (PAR) region of the electromagnetic spectrum (400–700 nm) the reflectance of vegetation is controlled by the absorption characteristics of pigments within leaves. The pigments which absorb the greatest proportion of radiation are chlorophyll *a* and *b* (referred to as Chl *a* and Chl *b* through the rest of this paper), which provide energy for the reactions of photosynthesis, and the carotenoids (referred to as Cars through the rest of this paper), which protect the reaction centres from excess light and help intercepting PAR as auxiliary

pigments of Chl *a*. Thus, changes in pigment concentrations relate strongly to the physiological status of a plant and therefore its productivity. Vegetation classification using remote sensing often relies upon multi-date measurements in order to capture the seasonal trend in reflectance, but the dependence upon phenological development is rarely expressed quantitatively. Very few studies consider the sensitivity of classification results to variations in canopy pigment composition through time, yet this may be a very useful source of additional information on the species present, as has been demonstrated for deciduous trees by Blackburn and Milton (1995).

Initially, when plants are subject to stresses, the changes in pigment concentrations may be relatively small, with more obvious changes in canopy structure. However, as stress levels increase further, complete foliar bleaching can result. While changes in the chlorophylls are indicative of stress and phenological stage, the concentration of Cars, provides complementary information on the physiological status of vegetation (Young and Britton 1990). In order to reveal this new information it will be necessary to derive new indices which are relatively insensitive to variations in canopy structure but show strong relations with plant pigment concentrations.

The fraction of PAR which is absorbed by a plant canopy (APAR) has been shown to be related to net primary productivity (NPP) as a function of an efficiency coefficient defining the carbon fixed per unit radiation intercepted (Monteith 1976). Several studies have demonstrated that measurements of canopy reflectance in the (chlorophyll-absorbing) red and the highly reflective near-infrared regions of the electro-magnetic spectrum (EMS) are linearly related to canopy APAR (Asrar *et al.* 1984, Sellers 1985, 1987). Therefore, it has been suggested that it is possible to use remotely sensed 'vegetation indices' to monitor temporal and spatial variations in APAR and relate this to NPP and CO_2 exchange (e.g., Fung *et al.* 1987, Bartlett *et al.* 1990). However, in such studies APAR is interpreted by assuming that the contribution of each pigment to the energetics of photosynthesis is equal. Research by Chappelle *et al.* (1992) and Kim *et al.* (1994) suggests that this is an insufficient interpretation, as the concentration of Chl *a* is the limiting factor in the utilisation of light for photosynthesis, because it receives energy absorbed by Chl *b* and the Cars. Thus, a situation may exist whereby APAR (as currently measured) is the same for two plants, but in the first plant the ratio of Chl *a* to Chl *b* and the Cars is higher than in the second. The first plant will have a higher photosynthetic potential than the second, despite both having the same APAR. Hence, APAR should be expressed as a function of the sum of the concentrations of the individual plant pigments.

In summary, the remote estimation of the concentration of individual pigments within plant canopies holds considerable potential for facilitating improved techniques for assessing the physiological status of vegetation (e.g., by detecting stress), for discriminating species (e.g., by monitoring phenological characteristics), and for estimating productivity (e.g., by measuring and interpreting APAR more accurately).

2.2. *Approaches to the remote estimation of pigment concentrations*

A wealth of studies have been undertaken to exploit the relations between the biophysical and biochemical properties of vegetation and its spectral reflectance properties. The most common practice has been to use the Normalised Difference Vegetation Index, a measure of the overall depth of the chlorophyll absorption feature in the red waveband, which has largely been used to estimate above-ground biomass and/or green leaf area index. This approach has been extended by using

more specific measurements of the shape of the chlorophyll absorption feature in hyperspectral data (e.g., Hall *et al.* 1990, Miller *et al.* 1990, Baret *et al.* 1992). Wessman *et al.* (1991) concluded that shape parameters such as width, depth, skewness and symmetry of absorption features are more indicative of biochemical state and canopy physiology than average reflectance over relatively broad spectral regions. However, there have been few investigations of the possibility of estimating the concentrations of photosynthetic pigments other than chlorophyll from measurements of spectral reflectance (e.g., Gamon *et al.* 1990).

The major problem in relating spectral reflectance to pigment concentrations is that different pigments absorb light in the same regions of the EMS, i.e., the absorption spectra of pigments are convoluted. Thus it is difficult to relate reflectance at any particular wavelength with the concentration of an individual pigment. In this respect, an approach by Chappelle *et al.* (1992) called the ratio analysis of reflectance spectra (RARS) holds promise. The technique was developed by defining narrow bands (6 nm) in the reflectance spectra of leaves which corresponded to unconvoluted absorption bands of Chl *a* and *b* and the Cars. These bands were identified by dividing a reference spectrum by a reflectance spectrum with a higher overall reflectance, producing a ratio spectrum which amplified spectral differences at wavelengths related to the pigment absorption bands. Ratios of reflectance in the selected narrow bands were found to correlate well with the concentrations of individual pigments within leaves. Hence it was possible to use RARS to accurately estimate the concentrations of Chl *a* and *b* and the Cars in soybean (*Glycine max*. Merr.) leaves using their measured reflectance spectra.

A similar technique has been developed by Peñuelas *et al.* (1995) to estimate the ratio between the foliar concentrations of the Cars and Chl *a*. It was found that the structure insensitive pigment index (SIPI), which employs ratios of reflectance at 800, 445 and 680 nm, can be used to accurately estimate the ratio of Cars to Chl *a*. The authors suggest that the SIPI minimises the effects of radiation interactions at the leaf surface and internal structures in the mesophyll, which can confound estimates of pigment concentration from reflectance spectra.

It is important therefore that the relative merits of such techniques are evaluated with respect to leaves of a range of species which have differing characteristics in terms of internal structures, surface characteristics and physiological condition.

3. Aims

This paper describes a laboratory-based study which forms the first part of a larger project investigating the potential of hyperspectral data for quantifying plant photosynthetic pigments. The aim of the present study was to determine the effectiveness of a number of spectral indices and waveband combinations for estimating the absolute and relative concentrations of photosynthetic pigments within deciduous tree leaves.

4. Methods

In order to use leaf samples with a wide range of pigment concentrations leaves were obtained from deciduous tree species on a series of occasions, at approximately weekly intervals, during the mature and senescent stages of their phenological cycle. The species investigated were Beech (*Fagus sylvatica*), Oak (*Quercus robur*), Maple (*Acer negundo*) and Sweet chestnut (*Castanea sativa*). The trees used for this experiment were in a mature woodland situated within half a mile of the laboratory.

Immediately after the leaf samples were detached from the trees they were taken to the laboratory for spectral reflectance measurements.

4.1. *Spectral measurements*

Spectral reflectance measurements were made using a Geophysical Environmental Research Corp. Single-Field-of-View IRIS (SIRIS) instrument loaned from the NERC Equipment Pool for Field Spectroscopy. This instrument is capable of measuring from 350 to 3000 nm but in this experiment only the visible and near-infrared portions of the spectra obtained were used and between 350 and 1000 nm the instrument has a spectral sampling interval of 2 nm and a spectral resolution of 4 nm. The spectral reflectance of each leaf was determined by placing it on a platform covered in black material, with the adaxial surface of the leaf upwards. Each leaf was pressed flat onto the surface in order to minimise variations in leaf orientation with respect to illumination and viewing angles. The experiment was conducted in a light-proof laboratory and the only source of illumination for the leaf was a 500 w Quartz-Halogen videolamp, with an illumination angle of 10°. The SIRIS sensor head was positioned at nadir, above the leaf in such a way that the field-of-view (FOV) of the instrument lay well within the perimeter of the leaf and a spectral scan was made. A measurement of the irradiance incident upon the leaf was then obtained by taking a reference spectrum of a Spectralon panel, placed in the same position as the leaf. Each target and reference scan pair were subsequently used to calculate a percentage reflectance spectrum, applying a calibration for the reflectance properties of the reference panel and corrections for the interference gratings within the instrument. Three reflectance spectra were obtained for each leaf, with the SIRIS FOV covering a different area of the leaf each time, and a mean spectrum was calculated. In order to minimise measurement error, each leaf was placed beneath the light source for the minimum time required to obtain the reflectance spectra, this avoided excessive drying-out and curling of the leaf samples.

4.2. *Pigment determinations*

On completion of spectral reflectance measurements, the leaf samples were immediately placed in sealed bags and frozen for short-term storage. As soon as was feasible pigment determinations were made for these samples. Leaf samples were weighed, crushed to form a homogenous slurry and mixed with Methanol (100 per cent pure solvent). A pinch of $MgCO_3$ was added to neutralise acids which can cause pigment decomposition and the mixture was placed in a refrigerator at $< 3°C$ for 24 hours. The samples were then centrifuged and filtered and the resultant extracts were made up to 50 ml by adding more solvent as required. The extracts were analysed using a Cecil Instruments 3020 Scanning Spectrophotometer. The analysis procedure was designed to minimise the time to completion after removing each leaf sample from the freezer. Therefore, excluding the 24 hr extraction time, the preparation and analysis procedure took approximately 10 minutes per sample. In addition, all procedures were carried out under low-light conditions in the laboratory in order to minimise photo-oxidation of pigments.

From the spectrophotometer data, absorbance values at 665·2, 652·4 and 470 nm were used to determine the concentrations of the extracted pigments using the

equations of Lichtenthaler (1987):

$$\text{Chlorophyll } a \ (C_a) = 16{\cdot}72A_{665{\cdot}2} + 9{\cdot}16A_{652{\cdot}4} \quad (1)$$

$$\text{Chlorophyll } b \ (C_b) = 34{\cdot}09A_{652{\cdot}4} + 15{\cdot}28A_{665{\cdot}2} \quad (2)$$

$$\text{Carotenoids } (C_{x+c}) = (1000A_{470} - 1{\cdot}63C_a - 104{\cdot}96C_b)/221 \quad (3)$$

The third equation gives the concentration of total Cars, i.e., the sum of the xanthophylls and β-carotene ($x + c$). These equations gave pigment concentrations per ml of extract which were converted to concentrations per unit leaf mass and subsequently per unit leaf area (mg m^{-2}).

4.3. *Specific leaf area determinations*

The specific leaf area (dry mass to area ratio) was determined for each species at each stage of senescence using additional samples of leaves obtained from the same branches as those used in the spectroradiometric sampling. Freshly picked leaves were weighed (fresh mass) then placed on a white sheet of paper and a sheet of clear perspex was placed on top of the leaves to keep them flat. A Logitech Scanman hand-held scanner, attached to a PC was then used to create a digital image of the leaves at 300 dpi resolution. A binary image of the leaves was created by applying a 50 per cent grey level threshold, which differentiated the leaves, which were represented as black pixels, from the white background. The number of black (leaf) pixels was counted using the AREA routine in the image processing/GIS package IDRISI and the area of the leaves was calculated based on a pixel size of $0{\cdot}0072\,\text{mm}^2$ (300 dpi). This technique for determining leaf area was tested by scanning pieces of black paper of different shapes and sizes which had a known area. An RMS error of 0·89 per cent was found for the technique which was considered acceptable. Following the scanning, the leaf samples were oven dried at 105° C until a constant mass was achieved (dry mass). The percentage moisture content of each leaf was calculated along with the specific leaf area. These values were used to calculate the area of leaf used for each pigment determination and hence the concentrations of pigments per unit leaf area.

5. Results and discussion

5.1. *Applying existing indices to reflectance spectra*

The following spectral indices were applied to the leaf reflectance data:

5.1.1. *Ratio analysis of reflectance spectra*

Chappelle *et al.* (1992) presented the following indices:

$$RARS_a = (R_{675}/R_{700})/(r_{670}/r_{700}) \quad (4)$$

$$RARS_b = (R_{675}/R_{650} \times R_{700}) \times (r_{650} \times r_{700}/r_{675}) \quad (5)$$

$$RARS_c = (R_{760}/R_{500})/(r_{760}/r_{500}) \quad (6)$$

where, R = percentage reflectance at the specified wavelength in the reflectance spectrum for any leaf i.e., R_{675} represents percentage reflectance at 675 nm, and r = percentage reflectance at the specified wavelength in the reference reflectance spectrum (in the present study this was the mean of 10 spectra of mature (i.e., pre-senescent) leaves with high pigment concentration). These equations use notation which is consistent with the present paper not that of Chappelle *et al.* (1992).

Chappelle *et al.* (1992) suggest that the wavelengths selected for these equations

represent the absorption maxima of Chl *a* (675 nm), Chl *b* (650 nm) and Cars (500 nm) which are least affected by convolution. Furthermore, they indicate that 700 nm represents the minima of Chl *a* absorption and 760 nm is where there is no further absorption of PAR and the slope towards increased reflectance is at a maximum (i.e., the red edge). Interestingly, in all spectra collected for the present study 760 nm was on the plateau region of high reflectance in the near-infrared, while 700 nm represented the mid-slope position of the red edge.

In the present experiment the RARS indices (as with all other indices tested) were calculated by using the values of percentage reflectance in the individual SIRIS channels which were centred on or closest to the specified wavelengths. The high spectral resolution of this instrument meant that the maximum distance between specified wavelength and the centre wavelength of the SIRIS channel used was never greater than 0·8 nm. The term 'waveband' is used in the remainder of this paper to describe a single SIRIS channel.

Figure 1 plots the RARS indices against pigment concentrations. The RARS*a* algorithm (figure 1 (*a*)) appears to show a highly non-linear response to Chl *a*. RARS*a* appears relatively insensitive to changes in Chl *a* concentrations above about $50\,mg\,m^{-2}$. At low Chl *a* concentrations ($<50\,mg\,m^{-2}$) RARS*a* shows a tendency to decrease with increasing Chl *a* concentration. This non-linear behaviour is contrary to Chappelle *et al.* (1992) who found a positive linear relation between RARS*a* and Chl *a*. A possible explanation for this discrepancy is that the leaf samples used in the present experiment had a range of Chl *a* concentrations which extended much lower (minimum $10\,mg\,m^{-2}$) than those used by Chappelle *et al.* (1992) (minimum approximately $200\,mg\,m^{-2}$). Indeed, if we observe the portion of the graph in figure 1 (*a*) which extends above $50\,mg\,m^{-2}$, there is some indication that RARS*a* has a positive linear relation with Chl *a*, however statistical analysis reveals only a weak correlation for this range of values (R^2 (coefficient of determination)$=0{\cdot}44$).

The form of the relation shown in figure 1 (*a*) can probably be explained by the fact that the RARS*a* index is responding to changes in the shape, position and magnitude of the red edge, as both wavebands used in this equation are on or very close to this spectral feature. For leaves with Chl (*a*) concentrations $>50\,mg\,m^{-2}$ we can suggest that these are mature or early senescent and subject to changes in leaf pigmentation but not yet affected by structural disintegration. This means that the characteristics of the red edge are largely being controlled by changes in reflectance in the red wavelengths. As senescence progresses and Chl *a* concentrations decline to very low levels ($<50\,mg\,m^{-2}$) the internal structure of the leaf breaks down. Now, the characteristics of the red edge become controlled by changes in the level of near-infrared reflectance as well as red reflectance. In other words, the RARS*a* index responds to Chl *a* concentrations until leaf structural changes become a more important controlling factor on the reflectance spectrum (or red edge specifically).

RARS*b* shows a strong linear relation with Chl *b*, in accordance with the findings of Chappelle *et al.* (1992). Moreover, despite the fact that four different species were used, at differing stages of senescence, a higher coefficient of determination was found in the present study ($R^2=0{\cdot}89$ compared to 0·817). In contrast, RARS*c* only exhibited a weak relation with Cars concentration, however the relation was positive and linear (as indicated in Chappelle *et al.* 1992) and the variability about the regression line does not appear to be systematic. As an experiment, a number of different reference spectra were used to calculate the RARS indices (*a*, *b* and *c*). The effect of this was to change the numerical relation between RARS and pigment concentration, but not to change the coefficient of determination.

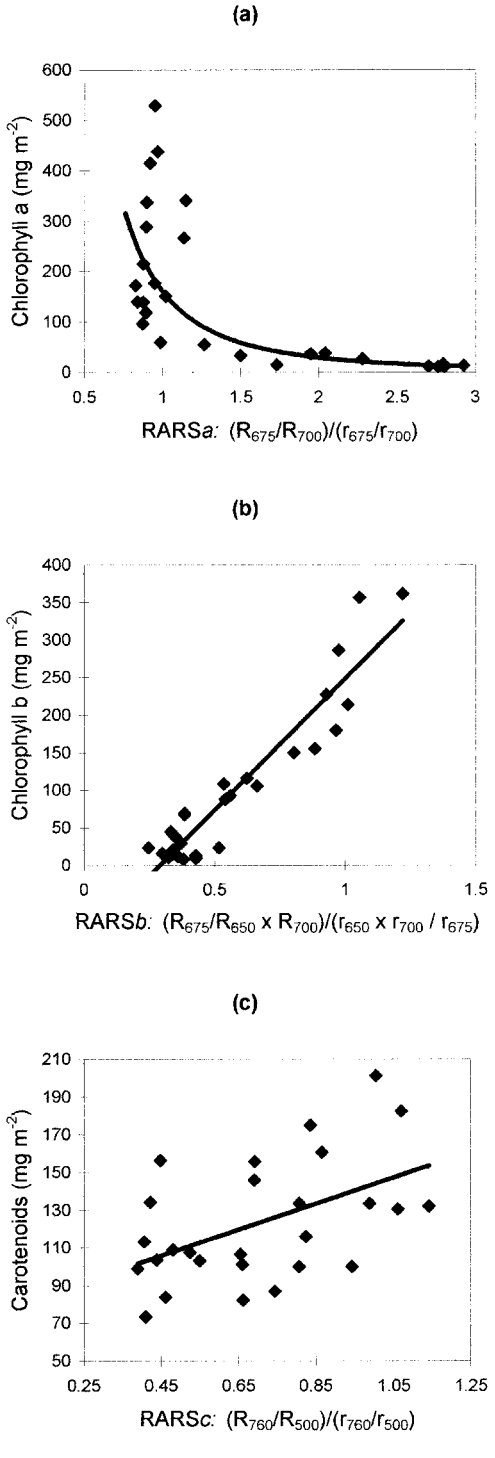

Figure 1. Relations between (*a*) RARS*a* and Chl *a*, best-fit regression model is $y = 161{\cdot}58x^{-2{\cdot}4817}$, $R^2 = 0{\cdot}7814$; (*b*) RARS*b* and Chl *b*, $y = 350{\cdot}7x - 102{\cdot}38$, $R^2 = 0{\cdot}8863$, and (*c*) RARS*c* and Cars, $y = 69{\cdot}217x + 74{\cdot}542$, $R^2 = 0{\cdot}2463$.

5.1.2. *Structure insensitive pigment index*

Peñuelas *et al.* (1995) presented the following index:

$$SIPI = (R_{800} - R_{445})/(R_{800} - R_{680}). \quad (7)$$

Peñuelas *et al.* (1995) found that this index, using these wavelengths, provided the best estimate of the ratio of Cars: Chl *a* for a range of leaves of different species and conditions. R_{800}, a near-infrared band was incorporated into the index to minimise the confounding effects of leaf structure. It was suggested that 680 and 445 nm correspond to the *in vivo* absorption maxima of Chl *a* and Cars respectively, though these wavelengths were selected empirically.

Figure 2 shows the results of the present experiment and confirms that SIPI has a curvilinear relation with the Cars: Chl *a* ratio which is best described using a logarithmic model (i.e., this model gives the highest coefficient of determination). SIPI lacks sensitivity for low values of Cars: Chl *a* and becomes more sensitive for higher values of the ratio, however, variability about the regression line also increases.

5.1.3. *Red-edge position*

The position of the red edge in each reflectance spectrum (RE) was identified as the wavelength of the peak in the corresponding derivative spectrum between 680 and 750 nm, i.e., the point of maximum slope. Several studies (e.g., Horler *et al.* 1983) have illustrated theoretically and empirically that RE can be used to estimate foliar chlorophyll content as an increase in pigment concentration will cause deepening and widening of the chlorophyll absorption feature. However, other work has shown considerable scatter around the RE-chlorophyll relation as a result of factors such as chlorophyll fluorescence (Lichtenhaler 1989), changing Chl *a*: *b* ratio (Rock *et al.* 1988) and the effects of secondary pigments (Curran *et al.* 1991).

Figure 3 shows that for the leaves used in this experiment there is a curvilinear relation between RE and Chl *a* concentration which is best described using a power model. Such a model can also be used to describe the relation between RE and Chl *b*, though with a slightly lower coefficient of determination ($R^2 = 0{\cdot}84$ compared

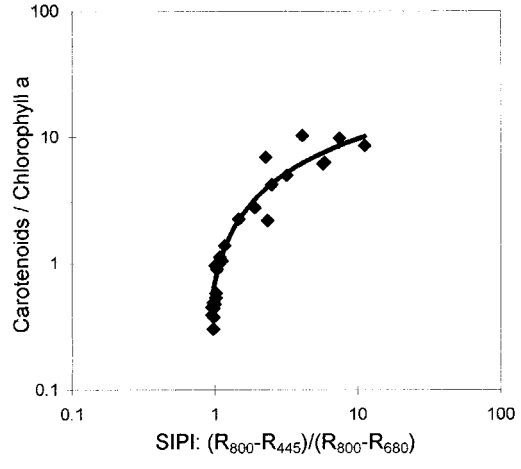

Figure 2. Relation between SIPI and the Cars: Chl *a* ratio (logarithmic axes are used in this graph in order to display the data more clearly and to be comparable with the plots of Peñuelas *et al.* 1995), $y = 3{\cdot}901 \mathrm{L}\, n(x) + 0{\cdot}7099$, $R^2 = 0{\cdot}8552$.

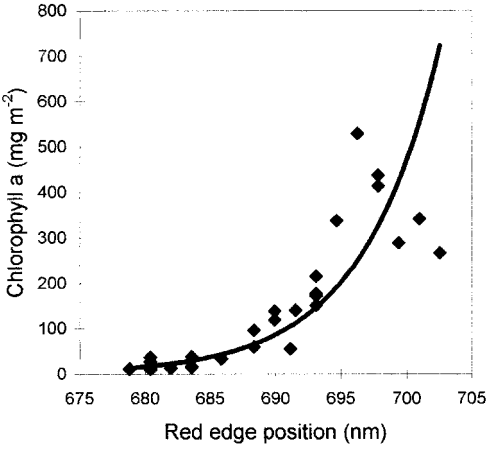

Figure 3. Relation between red edge position and Chl *a*, $y=2(10^{-49})e^{0{\cdot}1689x}$, $R^2=0{\cdot}8648$.

to 0·86 for Chl *a*). Interestingly, the scatter around the regression models appears to increase for higher chlorophyll concentrations. No relation was found between RE and Cars concentration which is to be entirely expected as the Cars only absorb in the blue wavelengths and therefore do not have an influence on the red edge.

5.2. *Applying new indices*

Following the intermediate success of existing spectral indices, two further indices were constructed and evaluated:

5.2.1. *Pigment specific simple ratio*

The following algorithms were used:

$$PSSR_a = R_{800}/R_{675} \tag{8}$$

$$PSSR_b = R_{800}/R_{650} \tag{9}$$

$$PSSR_c = R_{800}/R_{500} \tag{10}$$

The basis of this approach was to develop a simple spectral index for each pigment of interest, using a similar structure to that of the Simple Ratio Vegetation Index which itself is a measure of the overall depth of the chlorophyll absorption feature. Each index uses a near-infrared band (800 nm) which can be considered to minimise the effects of radiation interactions at the leaf surface and internal structures in the mesophyll, as suggested by Peñuelas *et al.* (1995). The wavebands 675, 650 and 500 nm were chosen on the basis of the suggestion by Chappelle *et al.* (1992) that these represent the absorption maxima of Chl *a*, Chl *b* and Cars, respectively, which are least affected by convolution.

When applied to the present data set, PSSR*a* has a strong relation with Chl *a* as does PSSR*b* with Chl *b*. A power model best describes both these relations giving coefficients of determination of 0·93 and 0·94 respectively and in both cases the variability about these models appears to increase with increasing pigment concentration. However, no relation was found between PSSR*c* and Cars concentration.

5.2.2. *Pigment specific normalised difference*

The following algorithms were used:

$$PSND_a = (R_{800} - R_{675})/(R_{800} + R_{675}) \quad (11)$$

$$PSND_b = (R_{800} - R_{650})/(R_{800} + R_{650}) \quad (12)$$

$$PSND_c + (R_{800} - R_{500})/(R_{800} + R_{500}) \quad (13)$$

This set of indices possess a structure analogous to that of the Normalised Difference Vegetation Index. As with PSSR, these indices incorporate a near-infrared band and use the pigment absorption maxima suggested by Chappelle *et al.* (1992). In this way the indices may provide a measure of the depth of the pigment absorption features in leaf spectra relative to the highly reflective near-infrared plateau. Applying these indices to the present data set we find that strong, exponential relations exist between PSND*a* and Chl *a* (R^2=0·90) and PSND*b* and Chl *b* (R^2=0·91), however no relation was found between PSND*c* and Cars.

5.3. *Identification of the 'optimum' wavebands for pigment indices*

As can be seen from the formulation of the RARS and SIPI indices, the selection of wavebands for pigment indices can vary considerably between workers. This may be accounted for by the fact that (*i*) the *in vitro* absorption maxima of pigments can shift by more than 20 nm depending on the polarity and water content of the solvent used, and (*ii*) the *in vivo* absorption maxima are difficult to determine because of the effects of convolution with other pigments. Moreover, the optimum wavebands for a pigment index, as determined empirically, may not necessarily be at the absorption maxima because here absorption may reach an asymptote (i.e., saturate) at fairly low pigment concentrations while wavebands along the wings of an absorption feature may continue to respond to further increases in pigment concentration.

For the present study, a step-wise regression analysis was undertaken in order to identify those wavebands (i.e., single SIRIS channel) at which reflectance was best correlated with the concentration of each of the photosynthetic pigments. Linear and curvilinear regression models were applied to the data sets and the optimum waveband was identified for each pigment. Chl *a* concentration was best correlated with reflectance at 680 nm, Chl *b* with 635 nm and Cars with 470 nm. These relations were all best described using power models as shown in figure 4. High coefficients of determination were obtained for the chlorophylls, while for Cars the regression model was only able to explain 49 per cent of the variability. For all of these relations there appears to be no systematic change in scatter around the regression model as pigment concentration changes.

If we consult published absorption spectra of isolated pigments, such as those of Lichtenthaler (1987) then it becomes possible to explain the above. Whatever the solvent used for spectrophotometric determinations, 680 nm is situated on the longer-wavelength wing of the Chl *a* absorption feature in the red region, where there is no absorption by Chl *b* or other pigments. In a similar fashion, 635 nm is situated on the shorter-wavelength wing of the Chl *b* absorption feature in the red region, where Chl *a* absorption is minimal. In other words, the optimum wavebands are on the wings of the pigment absorption features, which do not reach an asymptote (saturate) but remain sensitive through a range of pigment concentrations and are not convoluted by other pigments. For the Cars, 470 nm is on the longer-wavelength wing of the Cars absorption feature in the blue region, where there is no absorption

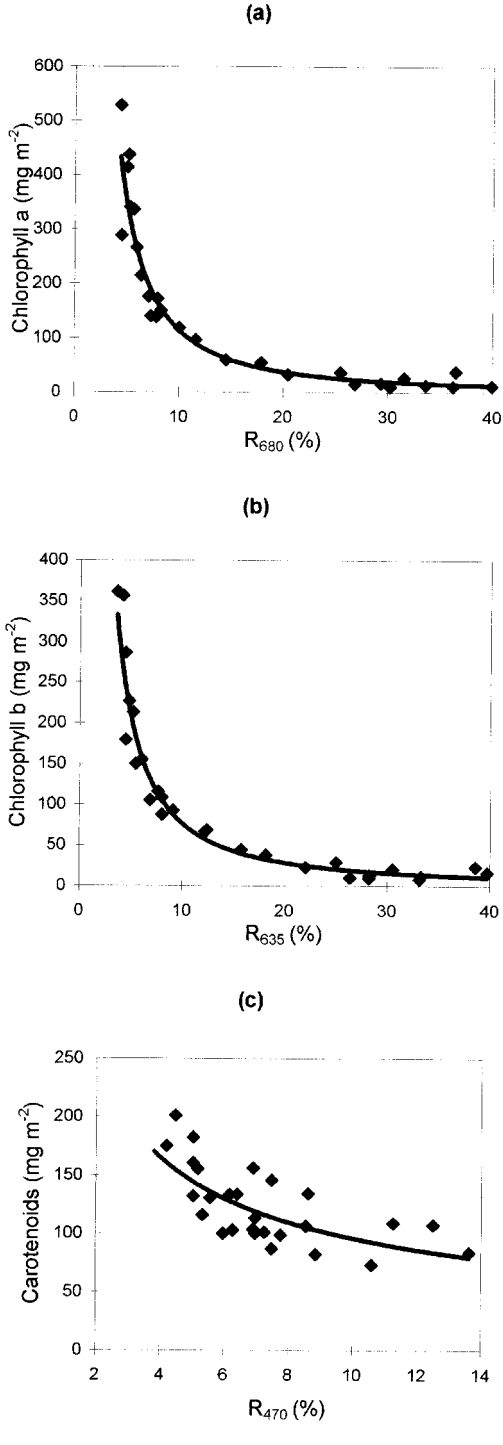

Figure 4. Relations between (*a*) R_{680} and Chl *a*, $y=4665{\cdot}2x^{-1{\cdot}6109}$, $R^2=0{\cdot}9413$; (*b*) R_{635} and Chl *b*, $y=2130{\cdot}2x^{-1{\cdot}4427}$, $R^2=0{\cdot}9338$; and (*c*) R_{470} and Cars, $y=378{\cdot}53x^{-0{\cdot}5961}$, $R^2=0{\cdot}4933$.

Table 1. Summary of results, illustrating, for each different formulation of a spectral index, the wavebands used in the algorithm, the pigment with which it was correlated, the regression model which best described the relation and the coefficient of determination for that relation.

Spectral index	Algorithm	Pigment	Regression model	R^2
RARS*a*	$(R_{675}/R_{700})/(r_{675}/r_{700})$	Chl *a*	$y=161{\cdot}58x^{-2{\cdot}4817}$	0·7814
	$(R_{680}/R_{700})/(r_{680}/r_{700})$	Chl *a*	$y=201{\cdot}71x^{-2{\cdot}75}$	0·8587
	$(R_{675}/R_{800})/(r_{675}/r_{800})$	Chl *a*	$y=303{\cdot}96x^{-1{\cdot}7156}$	0·9322
	$(R_{680}/R_{800})/(r_{680}/r_{800})$	Chl *a*	$y=337{\cdot}9x^{-1{\cdot}7588}$	0·9453
RARS*b*	$(R_{675}/R_{650}\times R_{700})\times(r_{650}\times r_{700}/r_{675})$	Chl *b*	$y=350{\cdot}7x-102{\cdot}38$	0·8863
	$(R_{680}/R_{635}\times R_{700})\times(r_{635}\times r_{700}/r_{680})$	Chl *b*	$y=353{\cdot}68x-106{\cdot}07$	0·9017
	$(R_{675}/R_{650}\times R_{800})\times(r_{650}\times r_{800}/r_{675})$	Chl *b*	$y=378{\cdot}8x-223{\cdot}73$	0·4821
	$(R_{680}/R_{635}\times R_{800})\times(r_{635}\times r_{800}/r_{680})$	Chl *b*	$y=354{\cdot}96x-209{\cdot}53$	0·4247
RARS*c*	$(R_{760}/R_{500})/(r_{760}/r_{500})$	Cars	$y=69{\cdot}217x+74{\cdot}542$	0·2463
	$(R_{760}/R_{470})/(r_{760}/r_{470})$	Cars	$y=109{\cdot}92x+26{\cdot}282$	0·2701
	$(R_{800}/R_{500})/(r_{800}/r_{500})$	Cars	$y=64{\cdot}117x+76{\cdot}546$	0·2202
	$(R_{800}/R_{470})/(r_{800}/r_{470})$	Cars	$y=111{\cdot}36x+24{\cdot}916$	0·2533
SIPI	$(R_{800}-R_{445})/(R_{800}-R_{680})$	Cars:Chl *a*	$y=3{\cdot}901\mathrm{L}\,n(x)+0{\cdot}7099$	0·8552
	$(R_{800}-R_{505})/(R_{800}-R_{690})$	Cars:Chl *a*	$y=3{\cdot}5919\mathrm{L}\,n(x)+0{\cdot}1507$	0·8534
	$(R_{800}-R_{470})/(R_{800}-R_{680})$	Cars:Chl *a*	$y=0{\cdot}9414\mathrm{L}\,n(x)+0{\cdot}6548$	0·8565

Table 1. (*continued*).

PSSR*a*	R_{800}/R_{675}	Chl *a*	$y=9{\cdot}4707x^{1{\cdot}7231}$	0·9322
	R_{800}/R_{680}	Chl *a*	$y=10{\cdot}928x^{1{\cdot}7691}$	0·9453
PSSR*b*	R_{800}/R_{650}	Chl *b*	$y=8{\cdot}4186x^{1{\cdot}5318}$	0·9405
	R_{800}/R_{635}	Chl *b*	$y=9{\cdot}1047x^{1{\cdot}6099}$	0·9530
PSSR*c*	R_{800}/R_{500}	Cars	$y=11{\cdot}089x+76{\cdot}546$	0·2202
	R_{800}/R_{470}	Cars	$y=17{\cdot}364x+24{\cdot}916$	0·2533
PSND*a*	$(R_{800}-R_{675})/(R_{800}+R_{675})$	Chl *a*	$y=7{\cdot}8648e^{4{\cdot}5725x}$	0·9034
	$(R_{800}-R_{680})/(R_{800}+R_{680})$	Chl *a*	$y=9{\cdot}4082e^{4{\cdot}5944x}$	0·9343
PSND*b*	$(R_{800}-R_{650})/(R_{800}+R_{650})$	Chl *b*	$y=6{\cdot}9136e^{4{\cdot}1753x}$	0·9105
	$(R_{800}-R_{635})/(R_{800}+R_{635})$	Chl *b*	$y=7{\cdot}5865e^{4{\cdot}3006x}$	0·9375
PSND*c*	$(R_{800}-R_{500})/(R_{800}+R_{500})$	Cars	$y=121{\cdot}43x+51{\cdot}642$	0·1878
	$(R_{800}-R_{470})/(R_{800}+R_{470})$	Cars	$y=341{\cdot}38x-113{\cdot}7$	0·2428
RE	λ of peak in 1st derivative	Chl *a*	$y=2(10^{-49})e^{0{\cdot}1689x}$	0·8648
RE	λ of peak in 1st derivative	Chl *b*	$y=6(10^{-45})e^{0{\cdot}1536x}$	0·8391
RE	λ of peak in 1st derivative	Cars	$y=1{\cdot}6557x-1020{\cdot}1$	0·1453
None	R_{680}	Chl *a*	$y=4665{\cdot}2x^{-1{\cdot}6109}$	0·9413
None	R_{635}	Chl *b*	$y=2130{\cdot}2x^{-1{\cdot}4427}$	0·9338
None	R_{470}	Cars	$y=378{\cdot}53x^{-0{\cdot}5961}$	0·4933

by Chl *a*. However, in solvents with a high water content (which may be the case *in vivo*), Chl *b* exhibits some absorption at this wavelength. This degree of convolution may explain why the relationship between reflectance at 470 nm and Cars concentration is weaker than those for the chlorophylls.

5.4. *Optimising the spectral indices*

While reflectance values in single wavebands may be closely correlated with pigment concentrations in this experiment, this may not be the case for whole vegetation canopies. One criticism could be that the step-wise regression techniques used can lead to 'over-fitting' of the data and to this end it is intended that the relations suggested in this study are evaluated against a test data set in the future. Moreover, in the field situation, variations in background reflectance properties, contributions from non-photosynthetic canopy components and the effects of leaf layering and canopy structure may weaken the relations between reflectance values in single wavebands and pigment concentrations. Pigment indices which use ratios of reflectance at different wavelengths (especially those which incorporate near-infrared wavebands) may overcome such difficulties, therefore, an attempt was made to identify the optimal waveband combinations for each spectral index. Each of the spectral indices was reformulated by systematically applying alternative sets of wavebands, including the three 'optimal' wavebands identified above. Once again, regression analysis was performed in order to define the relations between these modified indices and pigment concentrations. Table 1 summarises the results of this analysis, it does not include all the formulations of all the indices which were examined but does illustrate those formulations which produced the highest correlations with pigments or which are of interest for other reasons (the results for the analysis of RE and percentage reflectance (i.e., single bands) are also included for comparison).

With RARS*a*, the use of 680 nm (i.e., the 'optimum' waveband for Chl *a*) in place of 675 nm produced a notable increase in the strength of the relationship with Chl *a*. An even greater improvement was achieved by using 800 nm (on the near-infrared plateau) instead of 700 nm. The optimum configuration was obtained by replacing both of the original wavebands with 680 nm and 800 nm (figure 5). Here, the use of one waveband on the red edge and another, which is unaffected by Chl *a* absorption

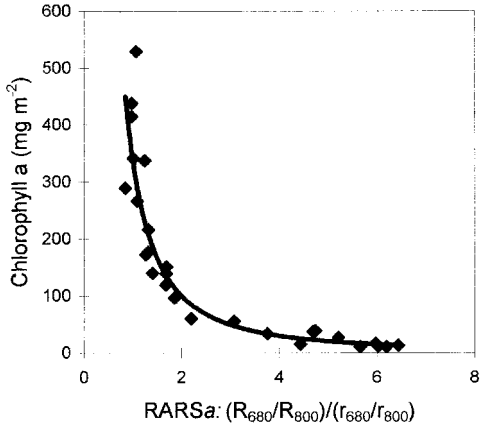

Figure 5. Relation between 'optimised' RARS*a* and Chl *a*, $y=337{\cdot}9x^{-1{\cdot}7588}$, $R^2=0{\cdot}9453$.

but responds to leaf structure, gave a much stronger relation with Chl *a* than using two wavebands on the red edge.

For RARS*b*, the use of 680 and 635 nm instead of 675 and 650 nm only slightly improved the relation with Chl *b* concentration, but the further modification of using 800 nm instead of 700 drastically reduced the correlation. Modifications to the RARS*c* index had little effect and no relations with Cars emerged. Similarly, no alternative waveband combinations were found to significantly improve the relations between the SIPI index and the Cars : Chl *a* ratio.

With both the PSSR and PSND indices, the use of the 'optimum' wavebands identified for each pigment produced a slight improvement in the correlations with pigment concentrations (figures 6 and 7). For both indices very high correlations were achieved for the chlorophylls but those for the Cars remain very low.

5.5. *Evaluation of the different indices*

Table 2 attempts to compare the various spectral indices and waveband combinations with respect to their correlation with pigment concentrations (the regression

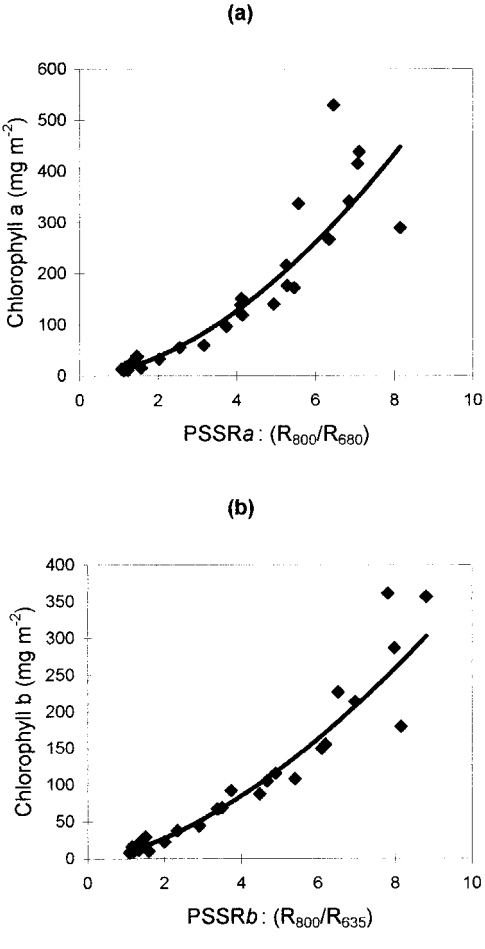

Figure 6. Relations between (*a*) 'optimised' PSSR*a* and Chl *a*, $y=10{\cdot}928x^{1{\cdot}7691}$, $R^2=0{\cdot}9453$; and (*b*) 'optimised' PSSR*b* and Chl *b*, $y=9{\cdot}1047x^{1{\cdot}6099}$, $R^2=0{\cdot}953$.

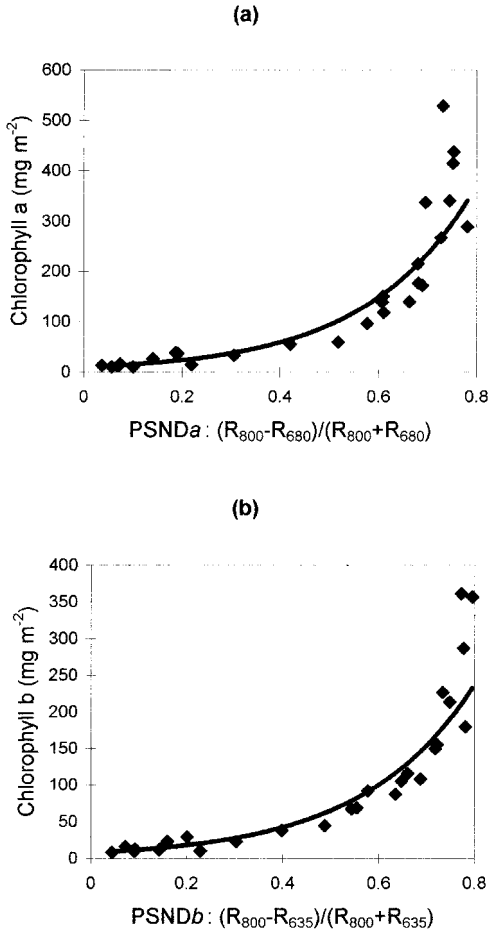

Figure 7. Relations between (*a*) 'optimised' PSND*a* and Chl *a*, $y=9{\cdot}4082e^{4{\cdot}5944x}$, $R^2=0{\cdot}9343$; and (*b*) 'optimised' PSND*b* and Chl *b*, $y=7{\cdot}5865e^{4{\cdot}3006x}$, $R^2=0{\cdot}9375$.

models used are given in table 1). For Chl *a*, the indices which appeared to have the best predictive capability were PSSR*a* and RARS*a*, both using the 'optimum' 680 nm waveband and 800 nm. The coefficient of determination was the same for both indices, confirming the fact that they were functionally identical (this is also the case for PSSR*c* and RARS*c*). While the RARS*a* index was highly sensitive at low Chl *a* concentrations it did reach an asymptote at around 200 mg m^{-2} (figure 5). PSSR*a* appeared better in this respect as its relation was more linear and it remained sensitive for high Chl *a* concentrations (figure 6 (*a*)). Most of the other indices and waveband combinations were also highly correlated with Chl *a*.

PSSR*b* was the index most highly correlated with Chl *b*, for both waveband combinations used. This index also appeared to remain sensitive to pigment fluctuations throughout the range of concentrations observed in this study (figure 6 (*b*)). In contrast, while they were highly correlated with Chl *b* concentration, PSND*b* and R_{635} had highly non-linear relations and were both only sensitive for low concentrations (figures 7 (*b*) and 4 (*b*)).

The highest correlation found for Cars was with R_{470}, which was much better

Table 2. Correlations between spectral indices and pigment concentrations, ranked by R^2.

Index	Algorithm	R^2
Chl *a*		
PSSR*a*	R_{800}/R_{680}	0·9453
RARS*a*	$(R_{680}/R_{800})/(r_{680}/r_{800})$	0·9453
None	R_{680}	0·9413
PSND*a*	$(R_{800}-R_{680})/(R_{800}+R_{680})$	0·9343
PSSR*a*	R_{800}/R_{675}	0·9322
RARS*a*	$(R_{675}/R_{800})/(r_{675}/r_{800})$	0·9322
PSND*a*	$(R_{800}-R_{675})/(R_{800}+R_{675})$	0·9034
RE	Peak in 1st derivative	0·8648
RARS*a*	$(R_{680}/R_{700})/(r_{680}/r_{700})$	0·8587
RARS*a*	$(R_{675}/R_{700})/(r_{675}/r_{700})$	0·7814
Chl *b*		
PSSR*b*	R_{800}/R_{635}	0·9530
PSSR*b*	R_{800}/R_{650}	0·9405
PSND*b*	$(R_{800}-R_{635})/(R_{800}+R_{635})$	0·9375
None	R_{635}	0·9338
PSND*b*	$(R_{800}-R_{650})/(R_{800}+R_{650})$	0·9105
RARS*b*	$(R_{680}/R_{635}\times R_{700})\times(r_{635}\times r_{700}/r_{680})$	0·9017
RARS*b*	$(R_{675}/R_{650}\times R_{700})\times(r_{650}\times r_{700}/r_{675})$	0·8863
RE	Peak in 1st derivative	0·8391
RARS*b*	$(R_{675}/R_{650}\times R_{800})\times(r_{650}\times r_{800}/r_{675})$	0·4821
RARS*b*	$(R_{680}/R_{635}\times R_{800})\times(r_{635}\times r_{800}/r_{680})$	0·4247
Cars		
None	R_{470}	0·4933
RARS*c*	$(R_{760}/R_{470})/(r_{760}/r_{470})$	0·2701
PSSR*c*	R_{800}/R_{470}	0·2533
RARS*c*	$(R_{800}/R_{470})/(r_{800}/r_{470})$	0·2533
RARS*c*	$(R_{760}/R_{500})/(r_{760}/r_{500})$	0·2463
PSND*c*	$(R_{800}-R_{470})/(R_{800}+R_{470})$	0·2428
PSSR*c*	R_{800}/R_{500}	0·2202
RARS*c*	$(R_{800}/R_{500})/(r_{800}/r_{500})$	0·2202
PSND*c*	$(R_{800}-R_{500})/(R_{800}+R_{500})$	0·1878
RE	Peak in 1st derivative	0·1453

than other spectral indices relatively, but this was still a weak relation in absolute terms. One explanation for this, as suggested earlier may be that R_{470} suffers convolution from Chl *b*. In addition, the relations for Cars may be much weaker than those for the chlorophylls because the range of Cars concentrations experienced in this study (201–73 mg m^{-2}) was much less than that for Chl *a* (529–10 mg m^{-2}) or Chl *b* (361–8 mg m^{-2}), by virtue of the leaf samples used. Such problems may be related to, or compounded by, limitations in the spectral resolution, radiometric sensitivity and signal-to-noise ratio of the GER-SIRIS and further work is needed to examine the technical requirements of an instrument in this context. Furthermore, it may be the case that as the leaves used in this experiment were at different stages of senescence, the relative proportions of the individual carotenoid pigments (e.g., β-carotene, lutein, violaxanthin and neoxanthin) were variable. As these individual pigments have slightly different absorption characteristics then the absorption characteristics of the Cars as a whole may vary through senescence. This effect may

create the observed scatter in the relationship between spectral indices and Cars concentration.

It is worth noting that the outcome of an analysis using empirical methods such as regression tends to be dependant on the setting of the experiment (species used, laboratory set-up etc.) and this may account for some of the disparities between the results presented in this paper and those of previous workers. Again if our aim is to develop spectral indices which can be used operationally then this effect has to be evaluated and will be the subject of further studies.

6. Conclusions

For deciduous tree leaves at various stages of senescence, several spectral indices exhibited excellent predictive relationships for Chl *a* and *b* and were insensitive to species type. In terms of individual wavebands, these pigments were most highly correlated with reflectance at 680 and 635 nm respectively. When these wavebands were incorporated into existing spectral indices such as RARS, they appeared to improve the relationships with pigment concentration. The PSSR*a* (R_{800}/R_{680}) and PSSR*b* (R_{800}/R_{635}) indices developed in this study had the strongest and most linear relations with Chl *a* and Chl *b* concentrations respectively.

None of the spectral indices used showed a good relationship with Cars but of those tested R_{470} was by far the best. The poor relations could be attributable to (*i*) convolution of the Chl *b* and Cars absorption features; (*ii*) the relative lack of variation in Cars concentration in the samples used in this experiment, or (*iii*) changes in the relative proportions of the individual carotenoid pigments through leaf senescence. However, the SIPI did have a good correlation with the Car : Chl *a* ratio, and was equally effective with a number of different waveband combinations.

Many of the spectral indices used were functionally similar and, because of spectral autocorrelation, their effectiveness changed little by using different wavebands. However, the results indicate that certain spectral indices and waveband combinations may be more sensitive, therefore more effective than others in some situations depending on the range of pigment concentrations experienced. It is now important that we investigate the applicability of the spectral indices described in this study at scales greater than the single leaf, from collections of leaves to whole vegetation canopies.

Acknowledgments

Many thanks to the NERC-Equipment Pool for Field Spectroscopy and its manager David Emery for the loan of the GER-SIRIS and invaluable assistance.

References

Asrar, G., Fuchs, B. M., Kanemasu, E. T., and Hatfield, J. L., 1984, Estimating absorbed photosynthetic radiation and leaf area index from spectral reflectance in wheat. *Agronomy Journal*, **76,** 300–306.

Baret, F., Jacquemond, S., Guyot, G., and Leprieur, C., 1992, Modelled analysis of the biophysical nature of spectral shifts and comparison with information content of broad bands. *Remote Sensing of Environment*, **41,** 133–142.

Bartlett, D. S., Whiting, G. J., and Hartman, J. L., 1990, Use of vegetation indices to estimate intercepted solar radiation and net carbon dioxide exchange of a grass canopy. *Remote Sensing of Environment*, **30,** 115–128.

Blackburn, G. A., and Milton, E. J., 1995, Seasonal variations in the spectral reflectance of deciduous tree canopies, *International Journal of Remote Sensing*, **16,** 709–721.

Chappelle, E. W., Kim, M. S., and McMurtrey, J. E., III, 1992, Ratio analysis of reflectance

spectra (RARS): an algorithm for the remote estimation of the concentrations of chlorophyll A, chlorophyll B and the carotenoids in soybean leaves. *Remote Sensing of Environment*, **39,** 239–247.

Curran, P. J., Dungan, J. L., Macler, B. A., and Plummer, S. E., 1991, The effect of red leaf pigment on the relationship between red-edge and chlorophyll concentration. *Remote Sensing of the Environment*, **35,** 69–75.

Fung, I. Y., Tucker, C. J., and Prentice, K. C., 1987, Application of advanced very high resolution radiometer vegetation index to study atmosphere-biosphere exchange of CO_2. *Journal of Geophysical Research*, **92,** 2999–3015.

Gamon, J. A., Field, C. B., Bilger, W., Bjorkman, A., Fredeen, A. L., and Peñuelas, J., 1990, Remote sensing of the xanthophyll cycle and chlorophyll fluorescence in sunflower leaves and canopies. *Oecologia*, **85,** 1–7.

Hall, F. G., Huemmrich, K. F., and Goward, S. N., 1990, Use of narrow-band spectra to estimate the fraction of absorbed photosynthetically active radiation. *Remote Sensing of Environment*, **32,** 47–54.

Horler, D. N. H., Dockray, M., and Barber, J., 1983, The red edge of plant leaf reflectance. *International Journal of Remote Sensing*, **4,** 273–288.

Kim, M. S., Daughtry, C. S. T., Chappelle, E. W., McMurtrey, J. E., and Walthall, C. L., 1994, The use of high spectral resolution bands for estimating absorbed photosynthetically active radiation. *Proceedings of the ISPRS Sixth International Colloquium on Physical Measurements and Signatures in Remote Sensing, Val d'Isère, France, 17–21 January 1994* (Paris: European Space Agency), pp. 299–306.

Lichtenthaler, H. K., 1987, Chlorophylls and carotenoids: pigments of photosynthetic membranes. *Methods in Enzymology*, **148,** 350–382.

Miller, J. R., Hare, E. W., and Wu, J., 1990, Quantitative characterisation of vegetation red edge reflectance. I. An inverted-Gaussian reflectance model. *International Journal of Remote Sensing*, **10,** 1755–1773.

Monteith, J. L., 1976, *Vegetation and the Atmosphere*, Vol. 2 (New York: Academic Press).

Peñuelas, J., Baret, F., and Filella, I., 1995, Semi-empirical indices to assess carotenoids/chlorophyll *a* ratio from leaf spectral reflectance. *Photosynthetica*, **31,** 221–230.

Rock, B. N., Hoshizaki, T., and Miller, J. R., 1988, Comparison of in situ and airborne spectral measurements of the blue shift associated with forest decline. *Remote Sensing of the Environment*, **24,** 109–127.

Sellers, P. J., 1985, Canopy reflectance, photosynthesis and transpiration. *International Journal of Remote Sensing*, **6,** 1335–1372.

Sellers, P. J., 1987, Canopy reflectance, photosynthesis and transpiration. II. The role of biophysics in the linearity of their interdependence. *Remote Sensing of Environment*, **21,** 143–183.

Young, A., and Britton, G., 1990, Carotenoids and stress. In: *Stress Responses in Plants: Adaptation and Acclimation Mechanisms*, edited by R. G. Alscher and J. R. Cumming (New York: Wiley-Liss), pp. 87–112.

Wessman, C. A., Ustin, S. L., Curtiss, B., and Gao, B. C., 1991, A conceptual framework for ecosystem modelling using remotely sensed inputs. *Proceedings of the ISPRS Fifth International Colloquium on Physical Measurements and Signatures in Remote Sensing, Courchevel, France, 17–21 January 1991* (Paris: European Space Agency), pp. 777–782.